SAND2022-8184C

Proceedings for the Fire and Climate Conference
May 23-27, 2022, Pasadena, California, USA and June 6-10, 2022, Melbourne, Australia
Published by the International Association of Wildland Fire, Missoula, Montana, USA

Peat Fires and Climate Change: Modeling Greenhouse Gas Emissions by 2100

Raquel S.P. Hakes*, Sagar Gautam, Matthew W. Kury, Umakant Mishra, Sarah N. Scott
Sandia National Laboratories[1], 7011 East Ave., Livermore, California, USA,
rshakes@sandia.gov, sgautam@sandia.gov, mwkury@sandia.gov, umishra@sandia.gov, snscott@sandia.gov

Rory M. Hadden
University of Edinburgh, Edinburgh, UK, r.hadden@ed.ac.uk

Mark J. Lara
University of Illinois, Urbana, Illinois, USA, mjlara@illinois.edu

Sara S. McAllister
United States Forest Service, Missoula, Montana, USA, sara.mcallister@usda.gov

Corresponding Author

Introduction

Smoldering of organic-rich "peat" soils is a key wildfire hazard across the globe. While peatlands make up less than 3% of the global land cover, they contain 25% of the terrestrial carbon store (Turquety *et al.* 2007), which can be released to the atmosphere if peat burns. As the climate warms, the frequency and severity of peat fires will increase, particularly in the Arctic, which is warming faster than the rest of the globe (Landrum and Holland 2020), and fire regimes may expand to include currently frozen tundra areas (Hugelius *et al.* 2020). Due to large uncertainties in estimating the mass of combusted peat, current estimates of peat fire emissions are highly uncertain (Rodríguez Vásquez *et al.* 2021). Previous work on computational modeling of peat fire burn depth has explored the effects of soil moisture content (MC), soil bulk density, and soil inorganic (mineral) content on ignition and smoldering of peat fires (Huang and Rein 2014; Huang *et al*. 2015; Huang and Rein 2015; Huang and Rein 2017). Here, we evaluate how changes in soil properties (i.e., MC, temperature, bulk density) resulting from climate change may impact the mass of peat burned within representative tundra ecosystems in Alaska.

Methods

Climate predictions

Model simulations project changes in air temperature and precipitation by 2100. Both these climatic factors affect soil MC and bulk density. Spatial ensemble-average values of air temperature and precipitation were calculated for the month of July (mid-fire season) under a high emissions scenario (SSP5-8.5) using outputs from four earth system models: CanESM

[1]Sandia National Laboratories is a multimission laboratory managed and operated by National Technology and Engineering Solutions of Sandia, LLC., a wholly owned subsidiary of Honeywell International, Inc., for the U.S. Department of Energy National Nuclear Security Administration under contract DE-NA0003525. SAND number.

(Swart *et al.* 2019), CESM (Danabasoglu *et al.* 2020), BCC (Wu *et al.* 2019), and UKESM (Senior *et al.* 2020). Air temperature increases across the state of Alaska for the period of 2071-2100 compared to 1992-2021 (Figure 1). Precipitation increases across the state in the month of July (Figure 1), though it varies inter-annually as some regions experience overall decreased precipitation.

Application to Alaska

We selected three climatically different peat dominated tundra ecosystems in Alaska as case studies. These locations include Deadhorse, the Kobuk River Delta, and the Yukon Kuskokwim Delta. The amount of temperature and precipitation change these locations may experience is shown in Figure 1. These sites also vary in soil properties such as average annual MC and soil bulk density. Table 1 shows the matrix of soil conditions used to parameterize the computational model for each location. For all locations, inorganic content is set to 12.7% (consistent with the kinetic parameters described in the literature), soil bulk density is kept constant at current values, and MC is varied from 1 to 40% to consider both unchanged, decreased, and increased MC. Comparing different soil densities gives us insight into the effects that future changes in soil bulk density will have on fire regimes and smoldering.

Table 1: Soil conditions for test locations.

	Deadhorse	Yukon Kuskokwim Delta	Kobuk River Delta
Soil bulk density (kg/m^3)	379	403	489
Current temperature (°C)	5.9	9.0	10.2
Future temperature (°C)	11.7	12.1	13.2

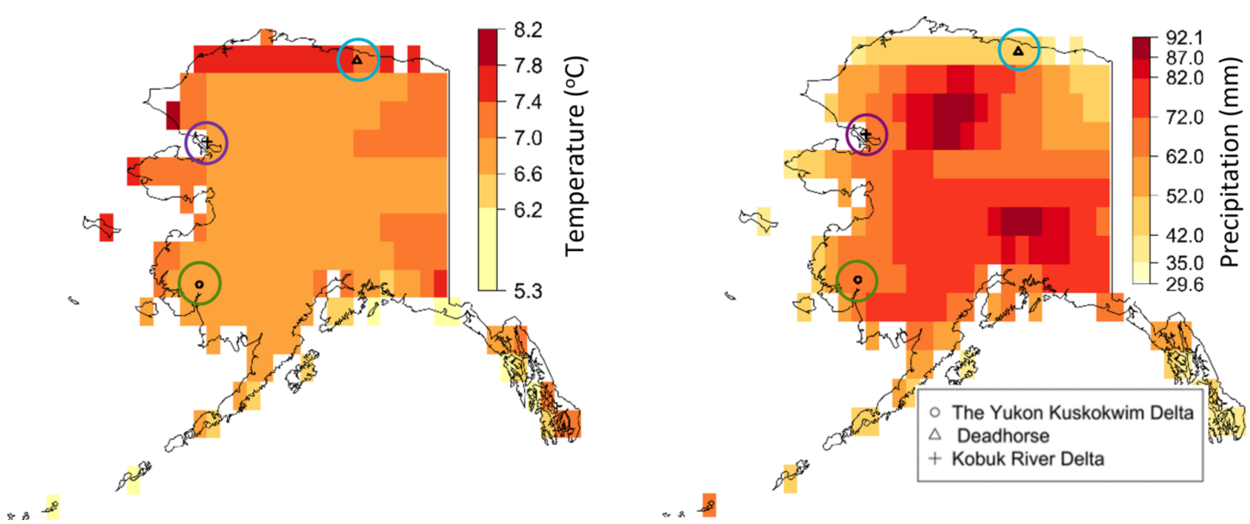

Figure 1: Case study locations in Alaska shown on maps of temperature change and precipitation change from present through 2100.

Computational methods

The quasi-1-D model used here is based on the work of Huang *et al.* (2015) and Huang and Rein (2015), in which a 1-D model of peat smoldering was developed in GPyro. A version of their model has been implemented in Sierra Thermal/Fluids: Aria (Notz *et al.* 2016). The ignition source is modelled as a 100 kW/m^2 flux applied to one end of the column for 300 s. Boundary conditions on the hot end and lateral sides assume radiative cooling to an ambient environment. Material properties of the solid phase species were taken from Huang and Rein (2015) with conductivity, porosity, and heats of reaction modified for the higher density peat considered here. A 5-step reaction mechanism, developed in Huang and Rein (2014), describes the peat smoldering process. We use kinetic parameters for Siberian transition-moor peat (Huang and Rein 2015). The model is run for 7,200 s on a column of peat 12 cm long. A 1-D problem is approximated in Aria by creating a mesh with elements in only one direction (i.e., a stack of blocks). The element edge length along the column of the peat is 0.8 mm. Time is advanced implicitly using adaptive time stepping, with a minimum of 1^{-9} s and a maximum of 1 s.

Results

Figure 2 shows the mass loss of peat over time, normalized by the mass of dry peat, for the Yukon Kuskokwim Delta. Temperatures in this narrow range have a negligible impact on mass loss. The change in slope (at 4500-5000 s) indicates the time that the column of peat is fully dried. Before this time (wet region), reactions include drying, pyrolysis, and oxidation; after this time (dry region), only pyrolysis and oxidation reactions occur. Comparing the end time of drying for different tests shows that reactions slow for higher MC soils.

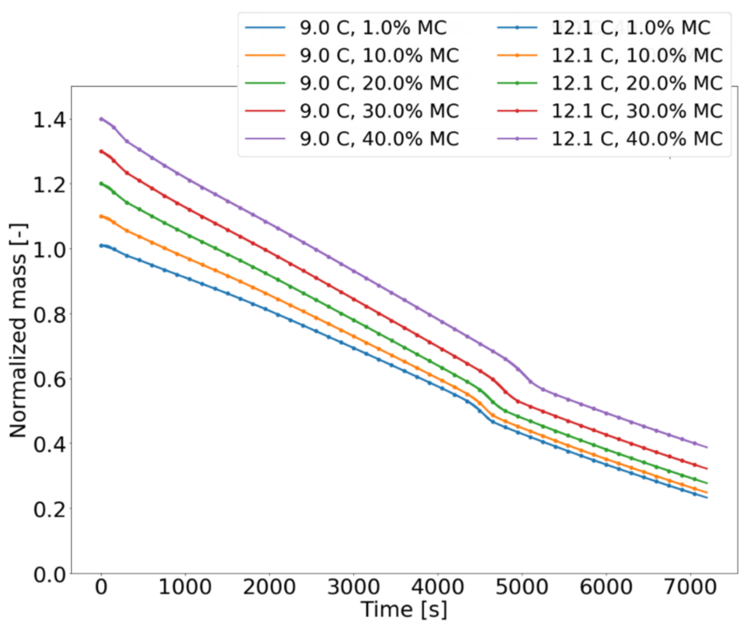

Figure 2: Mass loss normalized by mass of dry peat for Yukon Kuskokwim Delta simulations.

Similar results can be seen for the other locations. Figure 3 shows the steady state mass loss rate (MLR) values for the wet and dry regimes for all locations. MLR increases with soil bulk density and with MC. This trend is clearer for the wet soil (left) but remains even after the soil has completely dried (right). Clearly, the initial presence of water in the soil makes a difference, even after it dries. Note that the 30% and 40% MC Kobuk River Delta soil (the highest density soil) burned out after the igniter was turned off in the simulation.

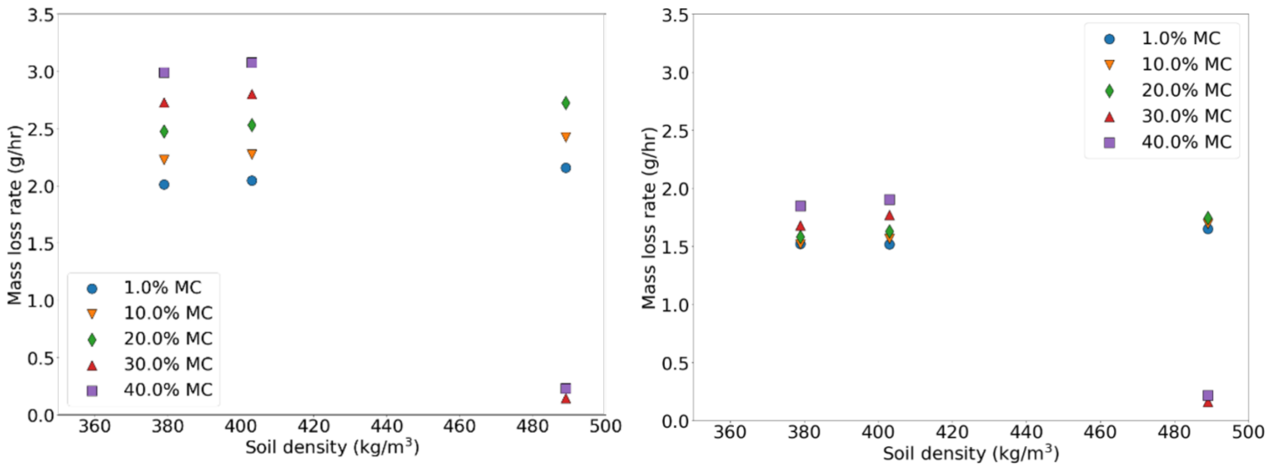

Figure 3: Steady state MLR in the (left) wet region, and (right) dry region for simulations at future temperatures.

The most useful parameter in relating mass loss to overall emissions is the total dry mass lost, shown in Figure 4. Total mass lost increases with increasing soil bulk density, as anticipated. While there is small variation in total mass lost with increasing MC, the lowest MC peat shows the highest mass loss. Additionally, the order of magnitude of the mass lost per unit area indicates substantial emissions when in-depth burning is considered.

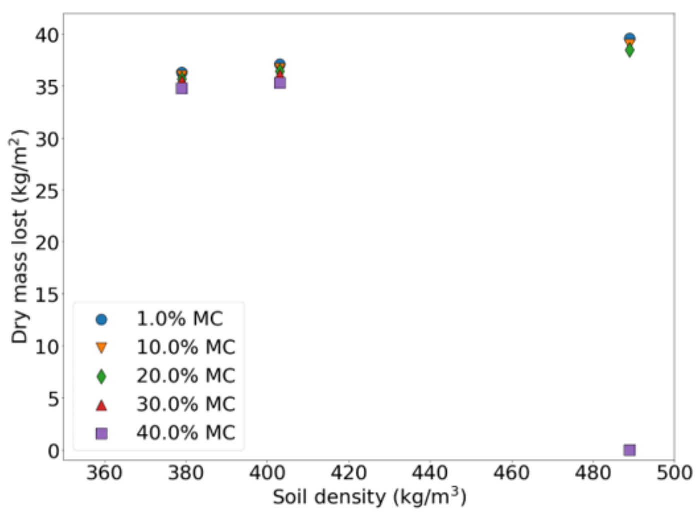

Figure 4: Total dry mass lost that can be converted to GHG emissions, for all locations.

Conclusions

Consistent with literature, both MC and bulk density have a clear impact on peat mass loss due to combustion. While soil temperature in the range considered here shows negligible impact on mass loss, it affects soil MC. We show that the total dry mass lost is large per unit area and will be directly tied to the emissions produced. Future work will explore the emissions of different GHGs and expand to boreal locations. Overall, the trends shown here provide insight on how to locate vulnerable peat soils as a function of both bulk density and MC, particularly as these conditions change with climate and fire.

Acknowledgements
Funding for the modeling portion of this work was provided by the Sandia LDRD program. This paper describes objective technical results and analysis. Any subjective views or opinions that might be expressed in the paper do not necessarily represent the views of the U.S. Department of Energy or the United States Government.

References

Danabasoglu G, *et al* (2020) The Community Earth System Model Version 2 (CESM2). *Journal of Advances in Modeling Earth Systems* **12**(2).

Huang X, Rein G (2014) Smoldering combustion of peat in wildfires: Inverse modelling of the drying and the thermal and oxidative decomposition kinetics. *Combustion and Flame* **161**: 1633-1644.

Huang X, *et al* (2015) Computational smoldering combustion: Predicting the roles of moisture and inert contents in peat wildfires. *Proceedings of the Combustion Institute* **35**: 2673-2681.

Huang X, Rein G (2015) Computational study of critical moisture and depth of burn in peat fires. *International Journal of Wildland Fire* **24**: 798-808.

Huang X, Rein G (2017) Downward spread of smouldering peat fire: the role of moisture, density and oxygen supply. *International Journal of Wildland Fire* **26**(11): 907-918.

Hugelius G, *et al* (2020) Large stocks of peatland carbon and nitrogen are vulnerable to permafrost thaw. *Proceedings of the National Academy of Sciences* **117**(34), 20438-20446.

Landrum L, Holland MM (2020) Extremes become routine in an emerging new Arctic. *Nature Climate Change* **10**(12), 1108-1115.

Notz PK, *et al*. (2016) 'SIERRA Multimechanics Module: Aria User Manual.' Sandia National Laboratories, Technical report. (Albuquerque, NM)

Rodríguez Vásquez MJ, *et al* (2021) Estimating Greenhouse Gas Emissions From Peat Combustion in Wildfires on Indonesian Peatlands, and Their Uncertainty. *Global Biogeochemical Cycles* **35**(2).

Senior CA, *et al* (2020) UK community Earth system modeling for CMIP6. *Journal of Advances in Modeling Earth Systems*, **12**(9).

Swart NC, *et al* (2019). The Canadian earth system model version 5 (CanESM5.0.3). *Geoscientific Model Development*, **12**(11), 4823-4873.

Turquety S, *et al*. (2007) Inventory of boreal fire emissions for North America in 2004: Importance of peat burning and pyroconvective injection. *Journal of Geophysical Research: Atmospheres* **112**(D12).

Wu T, *et al* (2019) The Beijing Climate Center climate system model (BCC-CSM): the main progress from CMIP5 to CMIP6. *Geoscientific Model Development* **12**(4), 1573-1600.